JOURNAL OF SPACECRAFT AND ROCKETS
Vol. 36, No. 6, November–December 1999

Orbit Transfer with a Variable Thrust Hall Thruster Under Drag

Y. Raitses*
Princeton University, Princeton, New Jersey 08543
M. Guelman†
Technion—Israel Institute of Technology, 32000 Haifa, Israel
and
J. Ashkenazy‡ and G. Appelbaum§
Soreq Nuclear Research Center, 81800 Yavne, Israel

The performance capabilities of an experimental Hall thruster were obtained experimentally for both variable and constant thrust modes at low power levels in order to enable orbit transfer under the influence of air drag with small satellites. For this purpose the measured thruster performance was employed in calculations of transfer trajectories. As a result, by applying optimal thrust acceleration control the required propellant mass for a given low-Earth-orbit transfer was reduced by 15–17% as compared to that required for spacecraft operation with a constant thrust to power ratio. For this purpose a Hall thruster with a movable anode is needed. In addition, the operation of an array of thrusters enables the increase of a factor of variations of the thrust acceleration during the flight time.

Nomenclature

a = semimajor axis, km
a_T = applied thrust acceleration, km/s^2
C_d = satellite drag coefficient
D = specific drag force, km/s^2
e = eccentricity
g = gravity, km/s^2
H = spacecraft altitude, km
h = angular momentum, km^2 rad/s
I_d = discharge current, A
I_{sp} = specific impulse, s
M = spacecraft mass, kg
$\dot{m}$ = mass flow rate, kg/s
P = electric input power, W
r = distance from the Earth's center to the satellite, kg
r_E = Earth's radius, 6378.14 km
S = effective cross-sectional area of satellite, km^2
T_{atm} = local atmosphere temperature, K
t = time (thrusting, mission), s
V_d = discharge voltage, V
v = spacecraft orbital velocity, km/s
$\boldsymbol{v}$ = velocity vector
W = ballistic coefficient, kg/km^2
β = reciprocal of the scale height, km^{-1}
Δt = time period of orbit changes, s
η = thruster efficiency
μ = Earth gravitational constant, 398,601.3 km^3/s^2
ρ = local atmospheric density, kg/km^3

Subscripts

f = final
m = mean
0 = initial

Presented as Paper 98-3487 at the AIAA/ASME/SAE/ASEE 34th Joint Propulsion Conference, Cleveland, OH, 13–15 July 1998; received 26 September 1998; revision received 14 June 1999; accepted for publication 14 June 1999.

*Researcher, P.O. Box 451, Princeton Plasma Physics Laboratory. Member AIAA.
†Professor, Asher Space Research Institute, Faculty of Aerospace Engineering.
‡Researcher, Propulsion Physics Laboratory. Member AIAA.
§Engineering Specialist, Propulsion Physics Laboratory.

Introduction

WITH the advent of paging and cellular and fiber communication networks, there is increasing interest in the use of low-Earth-orbit (LEO) small satellites (100–500 kg) for local and global satellite systems.[1] The main advantage of small satellites is their lower launch mass and, as a result, the spacecraft cost as compared to big and broadband LEO satellites. In addition to communication missions, small LEO satellites can also be useful for remote sensing.[2]

The problem with such applications of small satellites is that low-altitude orbits are considerably perturbed by the aerodynamic drag. For eccentric orbits ($e > 0$) orbital energy is lost because of the drag, resulting in the circularization of the orbit and a loss of altitude before reentry to the atmosphere occurs.[3] As a result, the satellite lifetime in LEO is limited. To overcome this limitation, a propulsion system has to be used. For this purpose high-I_{sp} electric thrusters enabling large propellant mass savings can be preferable to conventional chemical rockets.

The use of electric thrusters for space missions requires the presence of a constantly renewable onboard power source, which can represent a significant fraction of the initial spacecraft mass. On the other hand, the thrust acceleration applied to spacecraft is a function of the power; therefore, the limiting factor in the use of electric thrusters on small satellites is the electric power available for the thruster.

For many LEO space applications arcjet and resistojet thrusters are significantly superior to other types of electric thrusters because of their higher thrust to power ratio (0.1–0.5 N/kW) and typically smaller thruster mass for the same input power.[4–6] However, Hall electric thrusters can produce larger I_{sp} (1000–3000 s), as compared to these electrothermal thrusters, and achieve higher thrust densities ($\geq$1 mN/cm^2) than ion thrusters at a low power level from several hundred watts to a few kilowatts.[5] Because of these advantages, Hall thrusters can be useful for power limited LEO space missions such as on-orbit maneuvering and orbit transfer, which are not time critical or not limited in a number of maneuvers.[4] In addition to high thruster performance, an additional characteristics of Hall thrusters is that the jet velocity can, in principle, be modified independently on the input power and, therefore, the thrust can be controlled. This flexibility of Hall thruster performance can be useful to perform fuel optimal trajectories by applying a varying thrust acceleration to spacecraft during the flight time.[7]

The possibility of Hall thruster operation in a variable thrust mode was investigated.[8,9] For this purpose we used an experimental Hall thruster, which was developed and operated at Soreq.[10] A study of the effect of the thruster configuration, namely channel geometry and material, on Hall thruster operation enabled the modification of the experimental thruster and, as a result, the improvement of thruster performance.[9,11,12]

In the present paper we employed the two operating modes investigated with this modified thruster, namely, constant and variable thrust modes in order to implement orbit transfer in a resistive medium of a 200-kg Hall-thruster-propelled spacecraft. In addition, as an alternative to a constant thrust during the transfer time, a different approach of fuel optimal control, based on time-varying thrust acceleration, was used.[13] Representative examples of different transfer trajectories using either fuel optimal control or constant thrusting, and their impact on Hall thruster operation, are described and compared in this paper.

Fuel Optimal Control

In the case of Hall-thruster-propelled small satellites, we have a power limited system. According to Ref. 14, for this condition the optimal operating point of this system is to use maximum available electric power P_e. Then, the optimization criteria to minimize the propellant mass fraction f_p is to minimize the quadratic of the thruster acceleration applied to spacecraft $a_T \equiv T/M$, while keeping the thruster efficiency $\eta(\eta < 1)$ maximal[8]:

$$f_p \equiv \frac{\dot{m}t}{M} = \frac{M_f}{P_e}\int_{t_0}^{t_f} \frac{a_T^2}{\eta}\,\mathrm{d}t \qquad (1)$$

where t is the thrusting time during the mission. The thruster efficiency is the ratio of the thrust power to the input power given by

$$\eta = (T I_{sp}/2P_e)g \qquad (2)$$

Variable Thrust Hall Thruster

Thruster Output vs Input Parameters

A schematic drawing of the Hall thruster is shown in Fig. 1. The thruster has a coaxial geometry and consists of four main parts: anode, which is also a gas distributor, cathode-neutralizer, magnetic circuit, and a channel, made of an insulator material. The input electric power P_e is used in the electrical discharge between the two electrodes. The gas propellant, an inert gas, is injected into the channel through the anode and ionized by impact with the discharge electrons. The applied radial magnetic field, produced by the magnetic circuit, impedes the electron current toward the anode. This is what results in a significant axial electric field inside the discharge plasma. The plasma ions are accelerated by the electric field toward the channel exhaust resulting in the thrust.

At the Hall-thruster exit the accelerating ions acquire a kinetic energy proportional to the applied discharge voltage, and therefore specific impulse and thrust are given as

$$I_{sp} = T/\dot{m}g \propto \sqrt{V_d}, \qquad T \propto \dot{m}\sqrt{V_d} \qquad (3)$$

respectively. In addition, it follows from the principle of Hall-thruster operation that at the exit the discharge current I_d is essentially carried by the accelerating ions. Then, assuming effective single ionization of the propellant atoms and using the mass continuity, we can get

$$P_e = I_d V_d \propto \dot{m} V_d \qquad (4)$$

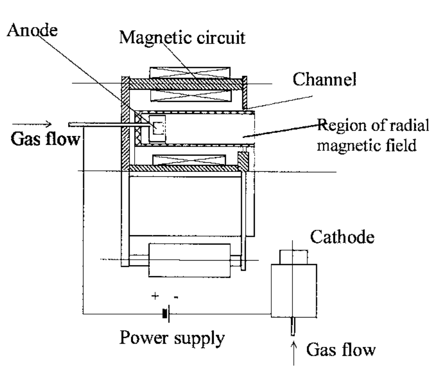

Fig. 1 Schematic drawing of the Hall thruster.

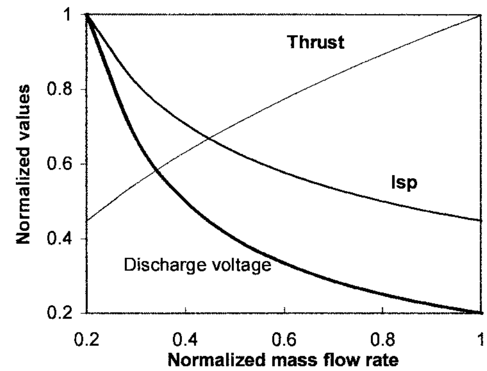

Fig. 2 Thrust, specific impulse, and discharge voltage vs the mass flow rate for a constant power and efficiency. All of these parameters are normalized to their maximum values.

To realize the optimal acceleration control, which was just explained, the thruster has to be operated in a variable thrust mode during the flight time. By using Eqs. (3) and (4), it is possible to derive the desired behavior of the specific impulse, the thrust and the discharge voltage vs the mass flow rate at a constant input power. Figure 2 shows such a behavior for a constant thruster efficiency.

As can be seen, Hall-thruster operation in a variable thrust mode requires modifications in both the mass flow rate and the discharge voltage. Obviously, to control thruster operation under these modifications, the electromagnetic coil current (magnetic field) must also be varied, too.[8]

Hall-Thruster Operation at Low Power Levels

To implement a low-power Hall thruster for spacecraft orbit control, two different operating modes can be used. These are either a constant thrust or a variable thrust mode. According to Ref. 5, existing Hall thrusters are scaled to operate at a constant thrust to power ratio, whereas their channel cross section is proportional to the input power. However, the thruster performance of smaller thrusters is lower than their large counterparts.[5] Moreover, it was suggested that an efficient variable thrust operation at a constant input power is not practical with the existing scaled down Hall thrusters.[8,9]

As an alternative to the conventional scaling of Hall-thruster geometry with the input power, a different approach was suggested in Ref. 9, based on laboratory thruster tests. These tests demonstrated ability to improve the ionization efficiency and, as a result, the performance at low power by varying the channel length and profile, but without scaling down the overall channel dimensions.[9] In addition, the suggestion was also made that in order to enable an efficient thruster operation at a variable thrust mode the thruster geometry must also be variable.[8]

We shall now apply some results measured with the laboratory thruster under the channel length variation to demonstrate the possibility of operating efficiently Hall thrusters in a variable thrust operating mode. Illustrative results in Figs. 3a–3c compare the thrust, specific impulse, and thruster efficiency vs the mass flow rate at an input power value of 415 ± 15 W, respectively, between the thruster with a fixed channel geometry for two different channel lengths ($L = 30$ and 40 mm) and a hypothetical thruster with a movable anode and, thus, with a variable channel length.[9] The thruster efficiency and specific impulse were obtained from the thrust, input power, and the anode mass flow rate measurements. The mass flow rate through the cathode, which is less than 10% of the anode mass flow rate, was not taken into account. The relative error in the thrust was determined as the ratio of the thrust stand resolution (0.5 mN) to the measured thrust magnitude. Then, taking into account the accuracy of mass flow rate and power measurements, the relative specific impulse and efficiency errors were obtained as the rms total static error.[9] For example, at the minimum thrust magnitude shown in

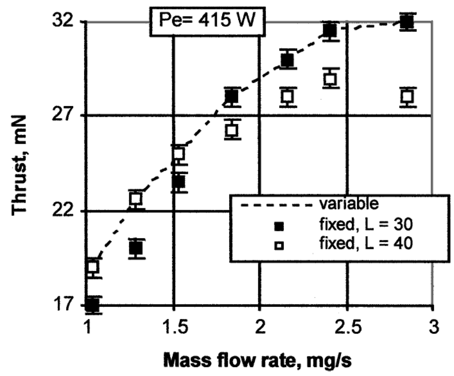

a) Thrust

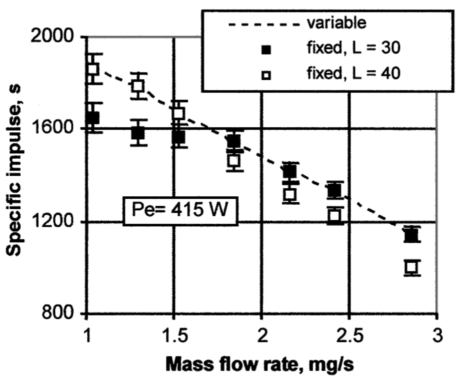

b) Specific impulse

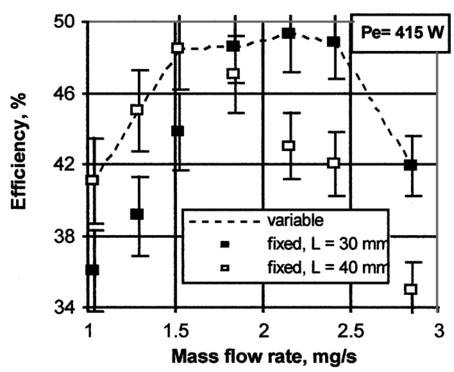

c) Efficiency vs the mass flow rate

Fig. 3 Hall-thruster operation at a constant input power of 415 ± 15 W and at a variable thrust mode with a fixed-channel geometry (L = 30 and 40 mm) and with a variable channel length.

Fig. 3a (17 mN), the relative thrust, specific impulse, and efficiency errors are about 3, 4, and 6.5%, respectively. The experimental setup including vacuum facility, thruster and diagnostic setup, and the experimental results are described in Refs. 8–12.

The points on the curves of Fig. 3 represent the measured performance with the laboratory thruster for different discharge voltage values. As the mass flow rate changes so does the discharge current, and thus the discharge voltage has to be changed in accordance to keep the input power constant (see Fig. 1).

As can be seen from these figures, there are overall improvements in thruster performance of the variable configuration as compared to the fixed one. Nevertheless, these improvements are in general not enough to maintain a high, constant thruster efficiency. In accordance with this result, the increase of the specific impulse, when the mass flow rate is reduced, is less than that expected from Eq. (3).

At low mass flow rates this degradation of the thruster performance can be attributed to wall losses that increase with the discharge voltage.[11] At mass flow rates larger than 2.1 mg/s, this behavior is most probably a result of ineffective ionization of the propellant at small discharge voltages causing a reduction of the thruster performance. In any case this behavior at high mass flow rates, which was observed at different values of the input power, may be an indication of a limitation to the increase in the mass flow rate and, as a result in the thrust variations, for a Hall-thruster operation in a variable thrust mode.

LEO Space Applications of Hall Thrusters

Atmospheric Drag Action on LEO Satellite

The loss of orbital energy by drag can be determined by $\mathrm{d}\boldsymbol{v}/\mathrm{d}t = \boldsymbol{D}$. This force acts along and opposite the spacecraft velocity vector

$$\boldsymbol{D} = -\delta \boldsymbol{v} \tag{5}$$

where

$$\delta = \tfrac{1}{2}(\rho v/W) \tag{6}$$

Here $W = M/SC_d$.

The density depends on the atmospheric composition and temperature and is reduced with height. In addition, the atmospheric density changes because of variations in solar input (day-to-night and solar activity variations). Because the atmospheric gases are usually described by the ideal-gas equation[3] and the vertical profiles of pressure and density can be determined by the use of the hydrostatic equation, the combination of these equations gives a simple relationship that describes the vertical atmospheric structure as

$$\rho = \rho_0 \exp(-\Delta H/\beta) \tag{7}$$

where $\beta = g/R_{\mathrm{atm}}T_{\mathrm{atm}}$, $\Delta H = H_f - H_0$, $H_0 = r_0 - r_E$, and R_{atm} is the local atmospheric gas constant.

To estimate roughly the time period Δt during which the loss of satellite altitude $\Delta H = r_0 - r_f$ occurs, it is helpful to regard the satellite orbit as circular ($e = 0$). Then the orbital velocity is determined by $v = (\mu/r)^{0.5}$. In addition, for simplicity, the atmospheric density is assumed to be constant in the band limited by ΔH and equal to the mean atmospheric density

$$\rho_m = \frac{1}{r_f - r_0}\int_{r_0}^{r_f} \rho\,\mathrm{d}r = \frac{1}{\beta}\frac{\rho_0 - \rho_f}{r_f - r_0} \tag{8}$$

In addition, the spacecraft velocity is also assumed to be constant and equal to the mean velocity

$$v_m = [2\mu/(r_0 + r_f)]^{0.5} \tag{9}$$

Using the virial theorem for a circular orbit[15] and equating the orbital loss to potential energy loss, we get the time period of changes in satellite altitude $\Delta H = \dot{r}\Delta t$ caused by atmospheric drag:

$$\Delta t \approx W \Delta H/\rho_m v_m r \tag{10}$$

For example, for the following satellite, orbit, and atmospheric parameters $W = 2\times10^7$ kg/km^2, $r = 6598$ km ($H_i = 220$ km), $\Delta H = 20$ km, $v_m = 7.78$ km/s, $\beta = 0.026$ km^{-1}, and $\rho_m = 0.22$ kg/km^3, an altitude loss of 20 km occurs in about 10 h. To prevent this attitude loss, the propulsion system has to produce the thrust magnitude equal to or greater than the drag force at the corresponding altitude.

Generally speaking, the drag effects just described have to be taken into account in the design of all of the spacecraft maneuvers, which take place in a resistive medium. These include, for example, transfer between neighboring circular orbits at low altitudes (for example, less than 300 km) where atmospheric drag effects are significant. The equations of motion of spacecraft are then given as follows[13]:

$$\dot{\boldsymbol{r}} = \boldsymbol{v}$$

$$\dot{\boldsymbol{v}} = a_T - \mu\boldsymbol{r}/r^3 + \boldsymbol{D} \tag{11}$$

To implement transfer between LEO orbits with a small satellite, a Hall-thruster propulsion system can be continuously operated at a constant input power during the transfer time, assuming of course the spacecraft power system can support it. Then, according to Eq. (1), applying thrust acceleration control enables the minimization of the propellant expenditure under the condition of a high-performance propulsion system.

Model of Orbit Transfer in a Resistive Medium

The problem of optimal transfer using power limited propulsion was treated, for example, in Refs. 13, 14, 16, and 17. In Ref. 13 a suboptimal thrust control for an electrically propelled spacecraft was defined for orbit transfer under the influence of air drag. In addition, this suboptimal control law was compared with the true optimum by employing a numerical algorithm to solve for the optimal transfer trajectory. The suboptimal fuel cost is only slightly greater than the true optimum.[13]

By using Eqs. (1) and (11) and employing the maximum principle,[15] the solution provided the optimal thrust acceleration enabling the minimization of the propellant expenditure defined as[13]

$$a_T = \{2/[c\exp(-\delta t) - 1]\}D \tag{12}$$

where c is the integration constant. By substituting this expression into Eq. (11), the spacecraft motion in polar coordinates and the orbital momentum $h = r^2\dot{\theta}$ are defined as follows:

$$r\ddot{\theta} + 2\dot{r}\dot{\theta} = -\{2/[c\exp(-\delta t) - 1] + 1\}\delta r\dot{\theta} \tag{13}$$

$$\ddot{r} - r\dot{\theta}^2 = -\mu/r^2 - \{2/[c\exp(-\delta t) - 1] + 1\}\delta\dot{r} \tag{14}$$

$$\dot{h} = -\{2/[c\exp(-\delta t) - 1] + 1\}\delta h \tag{15}$$

Following Ref. 13 in order to find c values for an extremal thrust acceleration, the atmospheric density is assumed constant and equal to ρ_m. Then, by using Eq. (15) for given initial and final altitudes of the circular orbits and the final transfer time t_f, the integration constant is obtained:

$$c = \frac{h_f^{\frac{1}{2}} - [h_0\exp(\delta_m t_f)]^{\frac{1}{2}}}{h_f^{\frac{1}{2}} - [h_0\exp(-\delta_m t_f)]^{\frac{1}{2}}} \tag{16}$$

The initial and final values of the angular momentum can be derived from the well-known orbital relations[3]

$$h = \sqrt{\mu a(1 - e^2)} \tag{17}$$

where a is the semimajor axis. In Eq. (16) δ_m is derived from Eq. (6) for $\rho = \rho_m$ and $v = v_m$. The orbital velocity is given by

$$v = \sqrt{\mu(2/r - 1/a)} \tag{18}$$

Then, by using Eqs. (16–18), the solutions of Eqs. (13–15) and, as a result, the behavior of the final semimajor axis and eccentricity under various t_f can be obtained. As a result, it is possible to find such values of the final time t_f^*, at which the spacecraft reaches a final orbit with a predesigned semimajor axis and eccentricity. As an example, we consider a LEO orbit transfer of a remote sensing spacecraft from an initial circular orbit with $r_0 = 6628$ km to a final circular orbit with $r_f = 6678$ km with the following orbital and spacecraft parameters: $\rho_0 = 0.0671$ kg/km^3, $\beta = 0.024$ km^{-1}, and $W = 2\times 10^7$ kg/km^2 (Ref. 13). In addition, the mean atmospheric density and the mean orbital velocity [see Eqs. (8) and (9)] are $\rho_m = 0.04$ kg/km^3 and $v_m = 7.74$ km/s, respectively.

Figure 4 shows an illustrative result estimated for the final eccentricity. As can be seen, the eccentricity is an oscillating function of the final time, whereas when it periodically reaches a zero value ($t_f = t_f^*$) the final orbit is circular. The same behavior was obtained for the final semimajor axis. Because the applied thrust acceleration is a time-dependent function [Eq. (12)], the required thrust level ($T = Ma_T$) during the transfer time is reduced with t_f^*. Then, by choosing the final time so that its proper value satisfies the limitations of thrust capabilities of a given propulsion system, optimal orbit transfer between, for example, circular orbits can be designed.

When considering the atmospheric density as an exponential function of orbital altitude [Eq. (7)] and drag forces proportional to the orbital velocity squared, the solutions of Eqs. (13) and (14) at

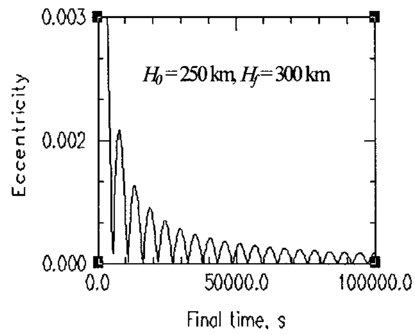

Fig. 4 Eccentricity vs the final time for orbit transfer with r_0 = 6628 km, r_f = 6678 km, the mean atmospheric density ρ_m = 0.0395 kg/km^3, and the mean velocity v_m = 7.74 km/s.

each time t are taken equal to those for transfer in an assumed constant density atmosphere from an actual orbit at t to a final orbit at t_f (Ref. 13). Then a suboptimal thrust acceleration and the resulting trajectories can be obtained by using actual values of the density, orbital velocity, and drag and by substituting $t_f - t$ instead of t_f into Eq. (16). In this case, in addition to the exponential term of Eq. (12), the integration constant is a time-dependent parameter. Therefore, for the transfer to be optimal the applied thrust acceleration must be varied. For this purpose the propulsion system has to operate at a variable thrust mode, and, therefore, the propellant expenditure will be affected by the behavior of the thruster efficiency [Eq. (1)] under various operating conditions.

To investigate the propellant mass and trajectory benefits of optimal thrust acceleration control, orbit transfer with a Hall-thruster propulsion system operated at a constant thrust mode was also considered. Because drag effects are maximal at the initial orbit, we assume that the constant thrust level is equal to the maximal thrust value, which is derived from Eq. (12) at $t = 0$. Then, by introducing Eq. (16) in Eq. (12) at $t = 0$, the value of the constant thrust can be obtained:

$$T_{\text{const}} = -\frac{2\left\{1 - [h_f\exp(\delta_m t_f)/h_0]^{\frac{1}{2}}\right\}}{\exp(-\delta_m t_f) - 1}M_s D_0 \tag{19}$$

where D_0 is the drag acceleration at the initial altitude and t_f is the final time obtained for the optimal transfer with the same initial and final orbital parameters.

In addition, the equations of spacecraft motion can be modified as follows:

$$r\ddot{\theta} + 2\dot{r}\dot{\theta} = -[(c+1)/(c-1)]\delta r\dot{\theta} \tag{20}$$

$$\ddot{r} - r\dot{\theta}^2 = -\mu/r^2 - [(c+1)/(c-1)]\delta\dot{r} \tag{21}$$

where the constant c is from Eq. (16) for the same orbit transfer with the applied acceleration control.

LEO Orbit with a Small Hall-Thruster Propelled Spacecraft

Based on experimental results with the laboratory thruster, the transfer of a 200-kg Hall-thruster-propelled satellite from an initial circular orbit ($e_0 = 0$) with radius $r_0 = 6598$ km ($H_0 = 220$ km) to a final orbit with $r_f = 6678$ km ($H_f = 300$ km) will be investigated.

The transfer will be performed by applying optimal thrust acceleration control and constant thrusting during the transfer time. For this purpose numerical simulations of orbit transfer use the results of Hall-thruster operation in both constant and variable thrust modes and for two different values of the constant input power, 320 and 500 W. To implement an efficient variable thrust operation, a hypothetical thruster with a movable anode is assumed.

In addition to two optimized missions of different power levels, two missions with constant thrusting at the same input power levels are performed within the same band of altitudes, 220 and 300 km. In each transfer case the propulsion system consists of two identical thrusters. Performance of the propulsion systems is given in Table 1. Here, the maximal thrust values are measured results of the thruster

Table 1 Operating parameters of two Hall-thruster propulsion systems for orbit transfer of a 200-kg spacecraft from H_0 = 220 km to H_f = 300 km[a]

Parameter	Two 320-W Hall thrusters	Two 500-W Hall thrusters
Total input power, W	640	1000
Total maximal thrust, mN	≥ 54	78
Factor of thrust variations (minimal to maximal thrust values ratio)	1.6	1.9

[a]Each propulsion system can be continuously operated in two different operating modes either with constant or variable thrust values.

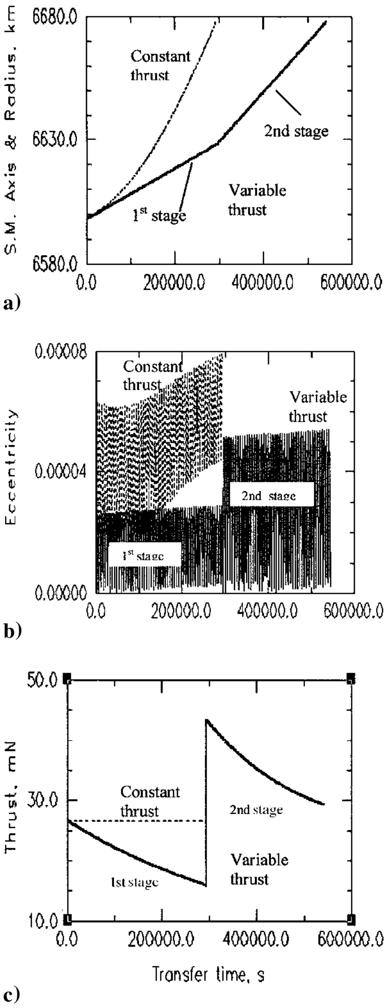

Fig. 5 LEO transfer of a 200-kg satellite between two circular orbits, H_0 = 220 km and H_f = 300 km, using two 320-W Hall thrusters operated at variable and constant thrust modes: a) semimajor axis and radius, b) eccentricity, and c) thrust of a single thruster. The transfer with a variable thrust is performed in two stages: in the first stage the thrust acceleration is generated by two thrusters, each operated 320 W, and at the second stage the thrust acceleration is generated by a single thruster operated at the input power of 640 W.

operation at large mass flow rates.[11] In addition, the minimal thrust values were measured at a small mass flow rate for the same channel case for $L = 40$ mm. The factor of thrust variations is taken as the ratio of maximal and minimal thrust values at a given input power.

Figures 5–8 show the numerical results for the semimajor axis and radius and eccentricity and operation of a single thruster vs the transfer time for the four representative transfer cases. The orbital parameters were obtained by solving equations of spacecraft motion: with optimal thrust acceleration [Eqs. (13) and (14)] and with the constant thrusting [Eqs. (20) and (21)]. To obtain the behavior of the thruster input parameters at different power levels, some experimentally obtained relations of the laboratory thruster were employed, namely, mass flow rate, discharge voltage, and the electromagnetic coils current vs the thrust. Finally, for each transfer case the required fuel mass was estimated from Eq. (1) taking into account changes in the thruster efficiency under various operating conditions at a constant input power. To compare the required fuel mass at each input power case, the final orbit of the optimal transfer was taken at the time when its orbital parameters are equal to those of the constant thrust transfer.

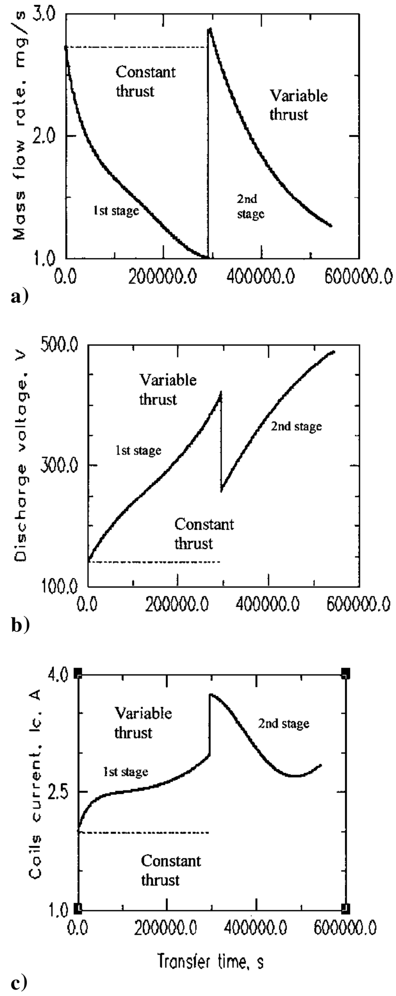

Fig. 6 Operation of a single Hall thruster during LEO transfer of a 200-kg satellite between two circular orbits, H_0 = 220 km and H_f = 300 km, at variable and constant thrust modes: a) mass flow rate, b) discharge voltage, and c) coils current. The transfer with a variable thrust is performed in two stages: first stage, the thrust is operated at the input power of 320 W, while at the second stage, at 640 W.

Transfer Using Two 320-W Thrusters

Figure 5 depicts these orbital parameters: semimajor axis and radius, eccentricity, and the thrust as function of time for the optimal transfer with a time-varying thrust and for the transfer with a constant thrusting. In both transfer cases the total input power available for the thrusters is 640 W. As in the case of a constant thrusting, the transfer with a time-varying thrust starts by applying full thrust, 53 mN, which is generated by two thrusters. Because the thrust variation capabilities at 320 W are not adequate to achieve the final orbit, the transfer is performed in two stages. In the first stage (220–250 km) optimal control is applied to both of these thrusters. The estimated final time of this stage is 294,400 s (3.4 days). At the second stage one of the thrusters is turned off, while the other thruster is operated at 640 W with a maximal thrust of 44 mN. Then, applying optimal thrust acceleration control enables the final orbit to be reached in about 3 days. The total fuel mass, which is required for both these stages (6.4 days), is 1.34 kg of xenon gas. Moreover, as can be seen from Fig. 5, the transfer with the constant thrusting is performed with two operating thrusters with the total thrust of

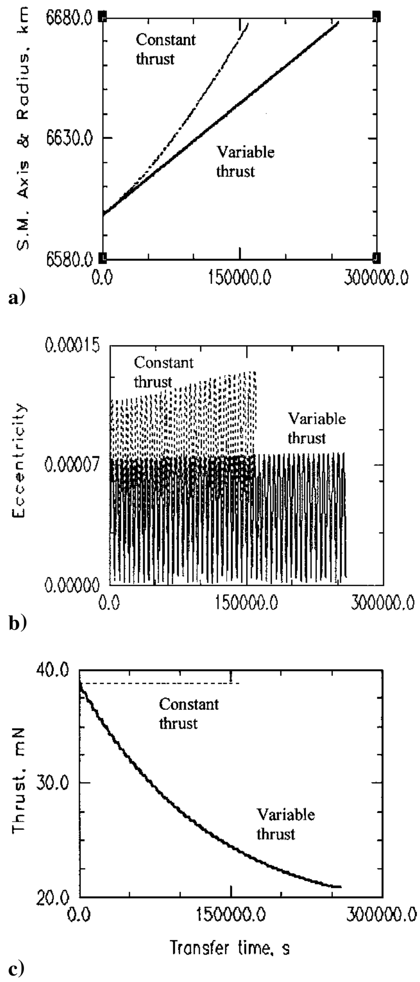

Fig. 7 LEO transfer of a 200-kg satellite between two circular orbits, H_0 = 220 km and H_f = 300 km, using two 500-W Hall thrusters operated at variable and constant thrust modes: a) semimajor axis and radius, b) eccentricity, and c) thrust of a single thruster.

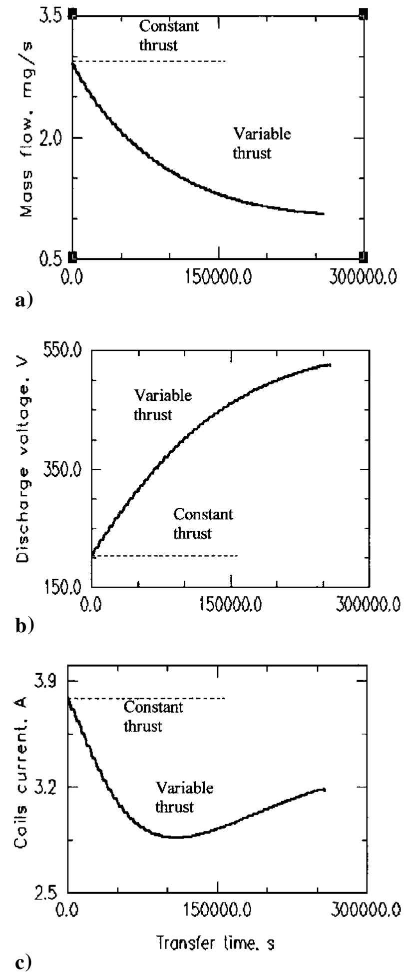

Fig. 8 Operation of a single 500-W Hall thruster during LEO transfer of a 200-kg satellite between two circular orbits, H_0 = 220 km and H_f = 300 km, at variable and constant thrust modes: a) mass flow rate, b) discharge voltage, and c) coils current.

53 mN. This transfer case requires about 3.4 days and 1.6 kg of xenon fuel.

Figure 6 shows the changes in the thruster input parameters, namely, the discharge voltage, mass flow rate, and coils current for a single thruster, which enable the implementation of the required time-varying thrust (Fig. 5c) during the transfer time. To provide an efficient thruster operation in both stages, the channel length is modified from $L = 30$ to 40 mm, as the mass flow rate through the thruster is reduced to 1.7 mg/s. The input power of each thruster during this stage is 320 W. At the end of the first stage, the channel length of the thruster, which is to be operated in the second stage, is returned to $L = 30$ mm. At this stage the input parameters of the operated thruster are changed to provide the time-varying thrust at 640 W.

Transfer Using Two 500-W Thrusters

For this input power case eccentricity, semimajor axis and radius, and thrust, all as the function of time, are shown in Figs. 7 and 8. Here, the orbital parameters and thrust changes are for two transfer cases: optimal and with constant thrusting. The performance and thrust variation capabilities measured with the laboratory thruster at 500 W enables the completion of the fuel optimal trajectory in one stage. Therefore, the time-varying thrust is generated by two 500-W thrusters up to the final orbit. The optimal transfer from $r_0 = 6598$ km to $r_f = 6678$ km is performed in 3 days.

This transfer requires 0.8 kg of xenon fuel. When a constant thrust of 39 mN $\times$ 2 is applied during the transfer time, the spacecraft achieves the final orbit in less than 2 days, whereas the required fuel mass for this mission is 0.95 kg.

Figure 8 shows the variations in the thruster input parameters of a single 500-W thruster for both transfer cases. In the case of a time-varying thrust, the channel length of both thrusters has to be changed only once (from $L = 30$ to 40 mm), when the mass flow rate is reduced to about 1.7 mg/s. As a result, the thruster efficiency is less affected by the mass flow rate variations, which are necessary to implement optimal acceleration control. For the transfer with a constant thrusting, the channel length is 30 mm. In addition, the input parameters, which are unchanged during the mission time, equal those obtained for the variable thrust case at the transfer start.

Conclusions

The performance capabilities of an experimental Hall thruster obtained for both variable and constant thrust modes at low power levels makes possible the implementation of orbit transfer under the influence of air drag with a small satellite. To effectively realize the propellant expenditure and trajectory benefits of a power limited optimization for LEO space missions with small spacecraft, the propulsion system could be based on a high efficiency Hall thruster with a variable channel geometry.

Based on the experimental results, the thruster performance of Hall thrusters tends to increase with the input power. Therefore the suggestion is made here that the required factor of thrust variations for a given space mission can be reduced by dividing the mission into multiple operating stages. If the total number of thrusters is determined by the initial value of the required thrust level and redundancy issues, the number of operating thrusters at different stages is reduced during the transfer, while the input power of each operating thruster is increased. The number of such stages can probably also be optimized with regard to minimum fuel mass by taking into account the performance capabilities of a given propulsion system. For example, the orbit transfer of a 200-kg Hall-thruster-propelled satellite from 220 to 300 km was investigated. For this purpose the measured results of the experimental Hall thruster were employed. By applying optimal acceleration control, the required propellant mass for the mission was reduced by 15–17% as compared to that required for spacecraft operation with a constant thrusting. For this purpose a Hall thruster with a movable anode is needed.

References

[1]Janson, S. W., "The On-Orbit Role of Electric Propulsion," AIAA Paper 93-2220, June 1993.

[2]Reale, J., "A Low Altitude Ion-Propelled Remote Sensing Spacecraft," International Electric Propulsion Conf., Paper 91-132, Oct. 1991.

[3]King-Hele, D., *Theory of Satellite Orbits in an Atmosphere*, 2nd ed., Butterworths, London, 1980, pp. 13–25.

[4]Butler, G. W., and Cassady, R. J., "Directions for Arcjet Technology Development," *Journal of Propulsion and Power*, Vol. 12, No. 6, 1996, pp. 1024–1036.

[5]Bugrova, A. I., Kim, V., Maslennikov, N. A., and Morozov, A. I., "Physical Processes and Characteristics of Stationary Plasma Thrusters with Closed Electron Drift," International Electric Propulsion Conf., Paper 91-079, Oct. 1991.

[6]Martinez-Sanchez, M., and Pollard, J. E., "Spacecraft Electric Propulsion-An Overview," *Journal of Propulsion and Power*, Vol. 14, No. 5, 1998, pp. 688–699.

[7]Guelman, M., Ashkenazy, J., and Raitses, Y., "From Earth to Moon with Electric Propulsion," International Astronautical Federation, Paper 94-A.6.050, Oct. 1994.

[8]Raitses, Y., Ashkenazy, J., and Guelman, M., "Hall Thruster Operation in a Variable Thrust Mode," *Proceedings of the 36th Israel Annual Conference on Aerospace Sciences*, Omanuth Press, Haifa, Israel, 1996, pp. 446–454.

[9]Raitses, Y., Ashkenazy, J., and Guelman, M., "Propellant Utilization in Hall Thrusters," *Journal of Propulsion and Power*, Vol. 14, No. 2, 1998, pp. 247–253.

[10]Ashkenazy, J., Raitses, Y., and Appelbaum, G., Investigations of a Laboratory Model Hall Thruster," AIAA Paper 95-2673, July 1995.

[11]Raitses, Y., Ashkenazy, J., Appelbaum, G., and Guelman, M., "Experimental Investigation of the Effect of Channel Material on Hall Thruster Characteristics," International Electric Propulsion Conf., Paper 97-056, Aug. 1997.

[12]Ashkenazy, J., Raitses, Y., and Appelbaum, G., "Parametric Studies of the Hall Current Plasma Thruster," *Physics of Plasmas*, Vol. 5, No. 5, 1998, pp. 2055–2063.

[13]Guelman, M., and Psiaki, M. L., "Electric Propulsion for Orbit Transfer in a Resistive Medium," *Journal of the Astronautical Sciences*, Vol. 44, No. 1, 1996, pp. 79–97.

[14]Marec, J. P., *Optimal Space Trajectories*, Elsevier, Amsterdam, 1979, pp. 7–19, 38.

[15]Goldstein, H., *Classical Mechanics*, 2nd ed., World Student Series, Addison Wesley Longman, Reading, MA, 1980, pp. 82–85.

[16]Gobetz, F. W., "Optimal Variable Thrust Transfer of a Power Limited Rocket Between Neighboring Circular Orbits," *AIAA Journal*, Vol. 2, No. 2, 1964, p. 369.

[17]Edelbaum, T. N., "Optimal Low Thrust Rendezvous and Station Keeping," *AIAA Journal*, Vol. 2, No. 7, 1964, pp. 1196–1201.

J. A. Martin
Associate Editor